

The Global Width Database for Large Rivers

(GWD-LR) version 1.2

Dai Yamazaki

JAMSTEC – Japan Agency for Marine Earth Science and Technology

d-yamazaki@jamstec.go.jp

1. Introduction

The Global Width Database for Large Rivers (GWD-LR) is a satellite-based global-scale database of river width [Yamazaki et al., 2014a]. GWD-LR is calculated from satellite water mask and flow direction map using fully-automated width calculation algorithm. The GWD-LR is freely distributed for research purposes. Please visit the GWD-LR webpage (<http://hydro.iis.u-tokyo.ac.jp/~yamadai/GWD-LR/index.html>). In order to acquire the password to download the GWD-LR, please e-mail to the developer (Dai Yamazaki).

Note that both the input dataset and the calculation algorithm has been updated from the previous versions. A brief description for river width calculation is available online

27 **2. Product Description**

28 The GWD-LR is prepared as a raster data. The data format is “plain binary” (i.e. Fortran
29 direct access, GrADS binary, ArcGIS BIL/BSQ/FLT format).

30 Effective river width (channel width excluding islands) is represented in the GWD-LR. A
31 land area <500 km² surrounded by water mask is treated as an island. River width is
32 calculated for each river centerline pixel, and the upstream-downstream relationships of
33 centerline pixels are given by flow direction maps. Therefore, river width data is available
34 sequentially along river networks.

35 The effective width data, flow directions, drainage area (and additional data such as
36 elevation) are prepared at three different resolutions.

37

38 **2.1 Original 3-sec resolution database**

39 River width is calculated at 3-sec resolution (about 90 m at the equator), and the
40 GWD-LR is available at the original 3-sec resolution. The data is divided into 5 degree by 5
41 degree tile (6000 pixels by 6000 pixels). Filename indicates the west and south corner of the
42 domain, e.g. **n30w140_wth.flt** is the width file for the domain of N30-N35, W140-W135.
43 Effective river width, flow direction map, drainage data is available in the original 3-sec
44 resolution database.

45 **[Effective River Width] \${LAT}\${LON}_wth.flt**

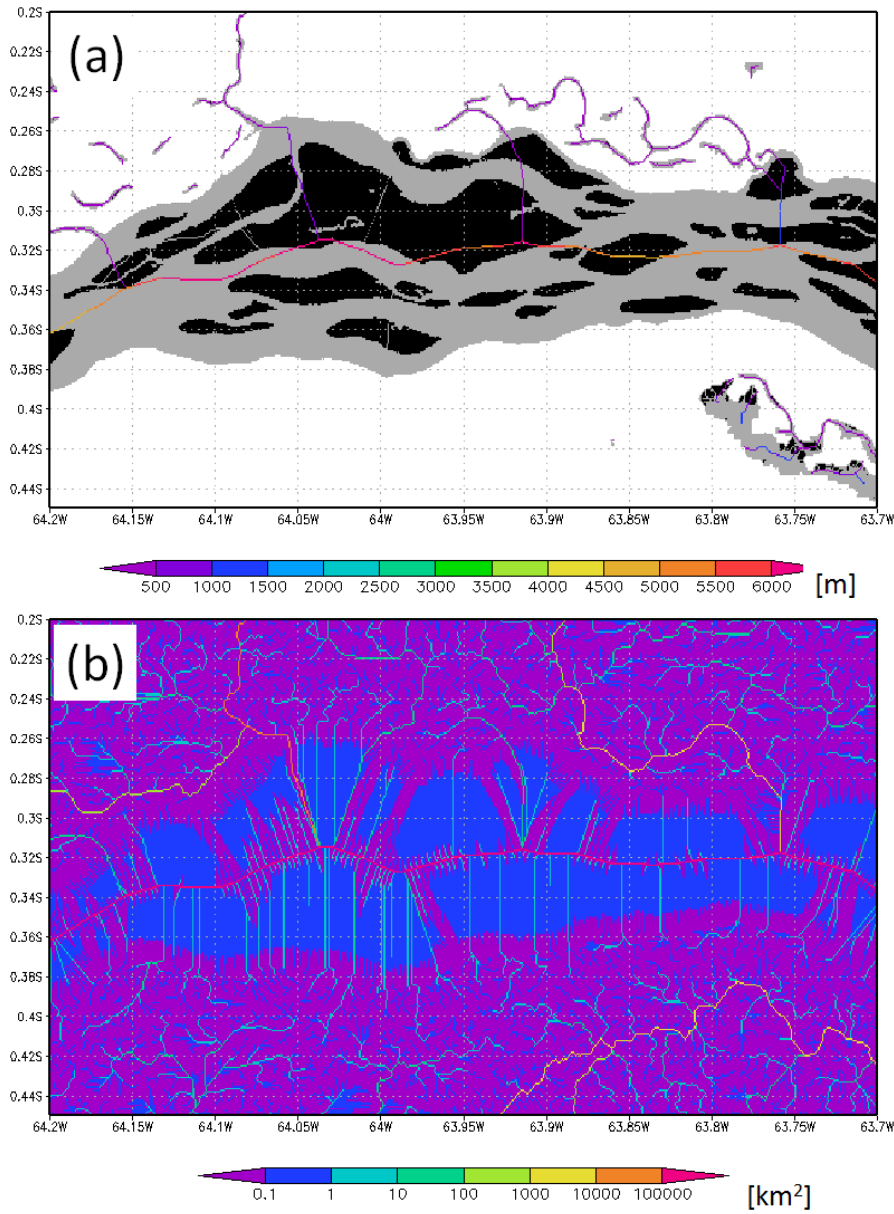
46 Effective river width (in [m], >0) is calculated for each centerline pixel. Land pixel,
47 non-centerline water pixel, and island pixel are represented by 0, -1, -2, respectively. Ocean
48 pixels are filled with undefined value (-9999). Data is prepared in 4 byte real format (in little
49 endian).

50 **[Flow Directions] \${LAT}\${LON}_dir.bil**

51 Flow direction of each pixel is represented by (1:N, 2:NE, 3:E, 4:SE, 5:S, 6:SW, 7:W,
52 8:NW). River mouth is represented by 0, while inland river terminating point is represented
53 by -1. Ocean pixels are filled by undefined value (-9). Flow direction is also a raster data,
54 thus all land pixels have a downstream direction. Note that the flow directions in GWD-LR is
55 modified from the original HydroSHEDS and GDBD flow directions, in order to represent the
56 centerline of each river segment. Flow direction map is prepared in 1 byte integer format.

57 [Drainage Area] \${LAT}\${LON}_upa.flt

58 Drainage area of each pixel is saved in [m²]. Ocean pixels are filled by undefined value
59 (-9999). Drainage area is saved in 4 byte real format in little endian.



60

61 **Figure 1: (a) Effective river width. Non-centerline water bodies are represented by gray,**
62 **while islands are represented by black. (b) Drainage Area of modified flow direction map.**

63 **2.2 Regional 0.005 degree resolution database**

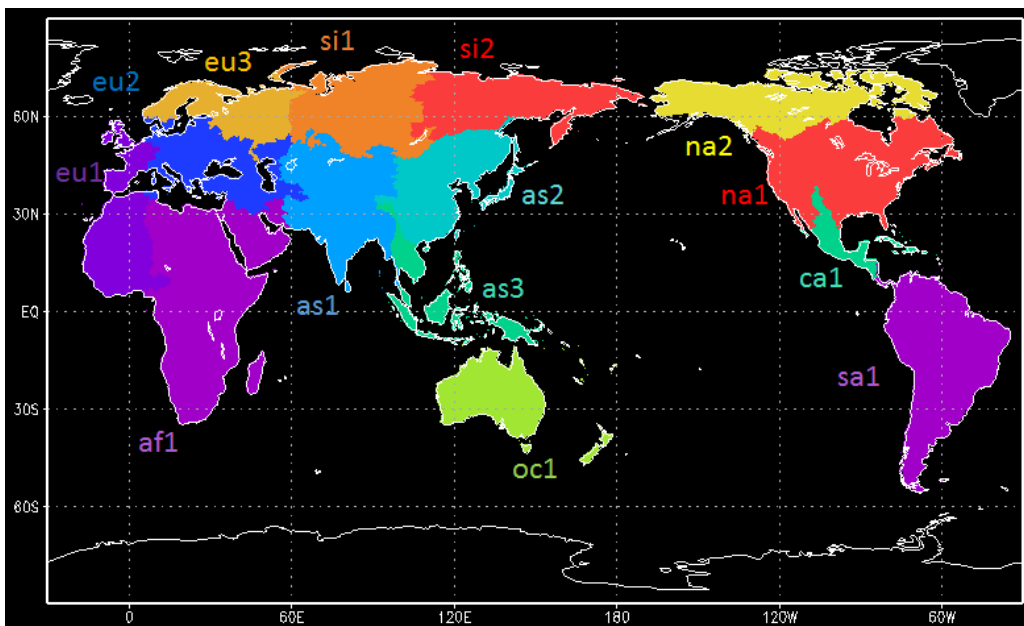
64 The original 3-sec resolution database was upscaled to 0.005 degree resolution by the
 65 FLOW algorithm [Yamazaki et al., 2009] in order to reduce the file size for easy data
 66 handling. The global domain is divided into 14 areas tagged by 3 characters.

67 **Table 1: List of areas in 0.005 degree resolution database**

Area Tag	sa1	ca1	na1	af1	eu1	eu2	as1
ID	1	2	3	4	5	6	7
West	-85	-120	-130	5	-20	5	55
East	-30	-60	-50	60	20	70	100
North	15	40	60	35	60	60	60
South	-60	5	25	-35	0	20	5
nx	11000	12000	16000	11000	8000	13000	9000
ny	15000	7000	7000	14000	12000	8000	11000
cell size	0.005	0.005	0.005	0.005	0.005	0.005	0.005

Area Tag	as2	as3	oc1	na2	eu3	si1	si2
ID	8	9	10	11	12	13	14
West	90	90	110	-170	0	55	100
East	150	155	180	-55	70	115	195
North	60	35	-10	75	80	80	75
South	20	-15	-50	50	45	45	50
nx	12000	13000	14000	23000	14000	12000	19000
ny	8000	10000	8000	5000	7000	7000	5000
cell size	0.005	0.005	0.005	0.005	0.005	0.005	0.005

68
 69 ID, domain boundary, number of cells, cell size are listed.



70
 71 **Figure 2: Areas for 0.005 degree resolution database.**

72 **[Effective River Width] \${AREA}.rivwth.flt**

73 Effective river width (in [m], >0) is calculated for each centerline cell. Land cell,
74 non-centerline water cell, and island cell are represented by 0, -1, -2, respectively. Ocean
75 cells are filled with undefined value (-9999). Data is prepared in 4 byte real format (in little
76 endian).

77 **[Downstream XY] \${AREA}.nextxy.bsq**

78 Downstream cell (jx,jy) of each cell (ix,iy) is saved. Record=1 represents downstream jx,
79 while record=2 represents downstream jy. River mouth is represented by -9. Ocean cells are
80 filled with undefined value (-9999). Data is prepared in 2 byte integer format.

81 The “downstream XY format” is used because upscaling of river network is
82 mathematically impossible when “D8 flow direction format” is used. For detail, see
83 [Yamazaki et al., 2009].

84 **[Drainage Area] \${AREA}.uparea.flt**

85 Drainage area of each cell is saved in [km²]. Ocean cells are filled by undefined value
86 (-9999). Drainage area is saved in 4 byte real format in little endian.

87 **[Adjusted Elevation] \${AREA}.elevtn.flt**

88 Elevation of each cell is saved. Ocean cells are filled by undefined value (-9999).
89 Elevation is saved in 4 byte real format in little endian.

90 Elevation is based on SRTM3 DEM (GTOPO30 DEM above 60N), and is adjusted
91 (smoothed) along river networks to remove depressions [Yamazaki et al., 2012].

92 **[Longitude / Latitude of outlet pixel] \${AREA}.lonlat.flt**

93 Longitude and latitude of the outlet of each pixel are saved. Record=1 is for longitude,
94 record=2 is for latitude. Longitude and latitude is saved in 4 byte real format in little endian.

95 Each 0.005 degree cell has 36 3-sec pixels. The outlet pixels of each cell represent the
96 position of river channel within the 0.005 degree cell.

97

98

99 **2.3 Global database (1/40, 1/10, 1/4 degree resolution)**

100 The 0.005 degree resolution database is again upscaled by the FLOW algorithm to
 101 construct global coverage database. Global database is prepared at various resolutions.
 102 This global database can be used in the global hydrodynamic model CaMa-Flood
 103 [Yamazaki et al., 2011, 2013, 2014b].

104 **[Effective River Width] width.flt**

105 Effective river width (in [m], >0) is calculated for each centerline grid. Land grid,
 106 non-centerline water grid, and island grid are represented by 0, -1, -2, respectively. Ocean
 107 grids are filled with undefined value (-9999). Data is prepared in 4 byte real format (in little
 108 endian).

109 **[Downstream XY] nextxy.bsq**

110 Downstream grid (jx,jy) of each grid (ix,iy) is saved. Record=1 represents downstream jx,
 111 while record=2 represents downstream jy. River mouth is represented by -9. Ocean grids
 112 are filled with undefined value (-9999). Data is prepared in 4 byte integer format.

113 **[Associated Maps]**

114 Global database contain files listed in the below table.

115 **Table 2: List of files in global domain database**

File	Description	Unit	Format
nextxy.bsq	Downstream X (rec=1) Downstream Y (rec=2)		integer
width.flt	GWD-LR Effective Width	[m]	real
elevtn.flt	Base Elevation	[m]	real
uparea.flt	Upstream Drainage Area	[m ²]	real
rivlen.flt	Channel Length	[m]	real
basin.bsq	Bain ID	-	integer
bsncol.bsq	Basin Color Patern for Visualization	-	integer
lonlat.flt	Outlet Longitude (rec=1) Outlet Latitude (rec=2)	deg deg	real real

117 Note: data format is 4 byte real or 4 byte integer, both in little endian.

118 **3. Input Data & Method**

119 **3.1 Flow Direction Map**

120 HydroSHEDS 3 arc-sec flow direction map [Lehner and Grill, 2013] is used as baseline
121 data between 60N and 60S. GDBD 1km flow direction [Masutomi et al., 2009] is used for
122 region above 60N. GDBD 1km flow direction map was downscaled to 3 arc-sec resolution,
123 and fused to HydroSHEDS flow direction map [Downscaling and fusing method: not
124 published yet]

125 **3.2 Water Mask**

126 SRTM Water Body Data (SWBD) [NASA/NGA, 2003] is used as baseline data between
127 60N and 60S. GLCF's MODIS Water Mask [Carrol et al., 2009] is used for region above 60N.
128 MODIS Water Mask is downscaled to 3 arc-sec resolution for calculating river width.

129 **3.3 Elevation Data**

130 For adding elevation to river network map, SRTM3 DEM (CSI version 4.1) [Reuter et al.,
131 2007; Farr et al., 2007] is used between 60N and 60S. The area above 60N is covered by
132 GTOPO30 [USGS]. Elevations are adjusted to remove depressions along river networks
133 [Yamazaki et al., 2012]. Then, integer-value elevations are converted to real-value in order
134 to smooth stepwise elevation increase due to integer representation [Smoothing method not
135 published yet].

136 **3.4 River Width Calculation**

137 Brief description on the width calculation algorithm is explained in Yamazaki et al., 2014a.
138 Detailed description document and sample source code are available online.

139 **3.5 Upscaling Method**

140 Flow direction and river width at 3 arc-sec resolution are upscaled to 0.005 degree
141 database by the FLOW algorithm [Yamazai et al., 2009]. Then, the 0.005 degree database
142 is again upscaled by the FLOW algorithm to create global database.

143

144

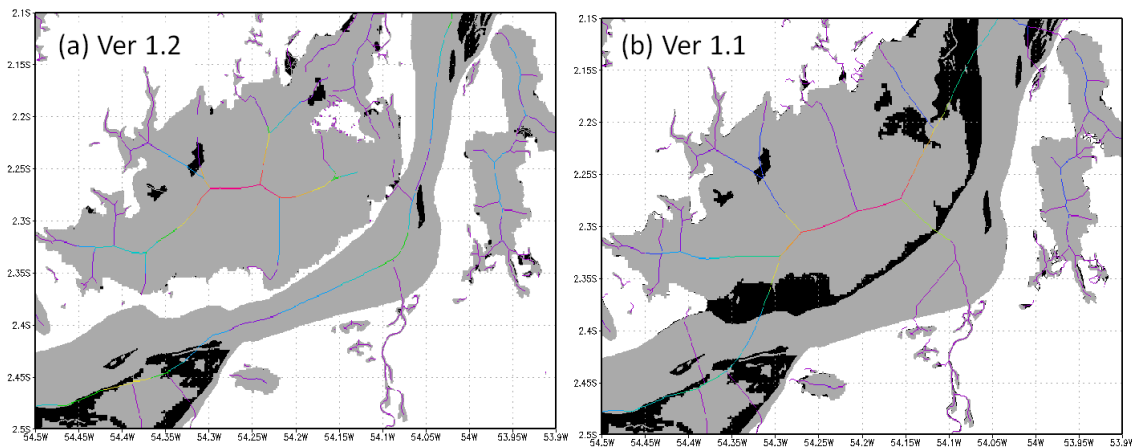
145 **4. Update in version 1.2**

146 **4.1 Database above 60N**

147 GWD-LR is extended to regions above 60N, using GDBD flow direction map and MODIS
148 water mask. Because low-resolution baseline data is used, the accuracy of river width is
149 lower in regions above 60N, compared to the accuracy between 60N and 60S.

150 **4.2 Channel/Floodplain Separation**

151 The algorithm is updated in version 1.2, and is now able to separate channels and
152 floodplains more strictly than the previous version. The accuracy of river width calculation is
153 improved.



154
155 **Figure 3: River centerlines calculated by (a) ver 1.2 algorithm and (b) ver 1.1 algorithm.**
156 **Channels and floodplains was not perfectly separated in version 1.1.**

157 **4.3 Seamless 3-sec resolution data**

158 In the previous version (ver. 1.1), the original 3-sec database is divided into 10 areas.
159 River width calculation algorithm is applied to global domain in version 1.2, thus 3-sec
160 resolution database (prepared as 5deg x 5deg tiles) has no area boundary.

161 **4.4 Parallelized Fortran90 code**

162 The width calculation algorithm was parallelized by OpenMP. Now, global calculation at
163 3-sec resolution can be done within one day. Previously, it took 3-4 days to finish global
164 calculation.

165 **5. Future Tasks**

166 **5.1 Lake Mask**

167 In GWD-LR, width is calculated for all water bodies, without separating river channels,
168 floodplains/wetlands, and lakes. This may not be ideal when GWD-LR is applied to
169 hydrodynamic model simulations or any other researches.

170 In order to distinguish river channels and lakes, a lake mask is currently under
171 construction.

172 **5.2 High-resolution water mask**

173 The accuracy of river width is low in the area above 60N because of low-resolution
174 MODIS water mask is used as baseline data. A new high-resolution water mask is under
175 development using LANDSAT GLS database.

176

177

178

179

180

181

182

183

184

185

186

187

188

189 **References**

- 190 Carroll, M. L., J. R. Townshend, C. M. Di Miceli, P. Noojipady, and R. A. Sohlberg (2009), A
191 new global raster water mask at 250 m resolution, *Int. J. Digital Earth*, 2(4), 291–308,
192 doi:10.1080/17538940902951401.
- 193 Farr, T. G., et al. (2007), The Shuttle Radar Topography Mission, *Rev. Geophys.*, 45,
194 RG2004, doi:10.1029/2005RG000183.
- 195 Lehner, B, and G. Grill (2013), Global river hydrography and network routing: baseline data
196 and new approaches to study the world's large river systems, *Hydrol. Proc.*, 27,
197 2171-2186, doi:10.1002/hyp.9740.
- 198 Masutomi, Y., Y. Inui, K. Takahashi, and U. Matsuoka (2009), Development of highly
199 accurate global polygonal drainage basin data, *Hydrol. Processes*, 23, 572 – 584,
200 doi:10.1002/hyp.7186.
- 201 NASA/NGA (2003), SRTM Water Body Data Product Specific Guidance, Version 2.0,
202 available online: http://dds.cr.usgs.gov/srtm/version2_1/SWBD/SWBD_Documentation/
- 203 Reuter H.I, A. Nelson, A. Jarvis (2007), An evaluation of void filling interpolation methods for
204 SRTM data, *International Journal of Geographic Information Science*, 21:9, 983-1008
- 205 Yamazaki, D., T. Oki, and S. Kanae (2009), Deriving a global river network map and its
206 sub-grid topographic characteristics from a fine resolution flow direction map, *Hydrol.*
207 *Earth Syst. Sci.*, 13, 2241 – 2251, doi:10.5194/hess-13-2241-2009.
- 208 Yamazaki, D., S. Kanae, H. Kim, and T. Oki (2011), A physically-based description of
209 floodplain inundation dynamics in a global river routing model, *Water Resour. Res.*, 47,
210 W04501, doi:10.1029/2010WR009726.
- 211 Yamazaki, D., C. Baugh, P. D. Bates, S. Kanae, D. E. Alsdorf, and T. Oki (2012), Adjustment
212 of a spaceborne DEM for use in floodplain hydrodynamic modeling, *J. Hydrol.*, 436-437,
213 81 – 91, doi:10.1016/j.jhydrol.2012.02.045.
- 214 Yamazaki, D., G. A. M. de Almeida, and P. D. Bates (2013), Improving computational
215 efficiency in global river models by implementing the local inertial flow equation and a
216 vector-based river network map, *Water Resour. Res.*, 49, 7221 – 7235,
217 doi:10.1002/wrcr.20552.
- 218 Yamazaki, D., F. O'Loughlin, M. A. Trigg, Z. F. Miller, T. M. Pavelsky, and P. D. Bates (2014a),
219 Development of the global width database for large rivers, *Water Resour. Res.*, 50,
220 doi:10.1002/2013WR014664.
- 221 Yamazaki, D., T. Sato, S. Kanae, Y. Hirabayashi, and P. D. Bates (2014b), Regional flood
222 dynamics in a bifurcating mega delta simulated in a global river model, *Geophys. Res.*
223 *Lett.*, 41, doi:10.1002/2014GL059744.